

Search on a Hypercubic Lattice through Quantum Random Walk: $d=2$

Apoorva Patel,^{1,2,*} K.S. Raghunathan,^{1,†} and Md. Aminoor Rahaman^{2,‡}

¹*Centre for High Energy Physics, Indian Institute of Science, Bangalore-560012, India*

²*Supercomputer Education and Research Centre, Indian Institute of Science, Bangalore-560012, India*
(Dated: May 31, 2019)

We investigate the spatial search problem on the two-dimensional square lattice, using the Dirac evolution operator discretised according to the staggered lattice fermion formalism. $d = 2$ is the critical dimension for the spatial search problem, where infrared divergence of the evolution operator leads to logarithmic factors in the scaling behaviour. As a result, the construction used in our accompanying article [1] provides an $O(\sqrt{N} \log N)$ algorithm, which is not optimal. The scaling behaviour can be improved to $O(\sqrt{N \log N})$ by cleverly controlling the massless Dirac evolution operator by an ancilla qubit, as proposed by Tulsi [4]. We reinterpret the ancilla control as introduction of an effective mass at the marked vertex, and optimise the proportionality constants of the scaling behaviour of the algorithm by numerically tuning the parameters.

PACS numbers: 03.67.Lx

I. TWO-DIMENSIONAL SPATIAL SEARCH

The spatial search problem is to find a marked object from a database spread over distinct locations, with the restriction that one can proceed from any location to only its neighbours while inspecting the objects. In our accompanying article [1], we have investigated the problem for $d > 2$ hypercubic lattices using the massless Dirac evolution operator, and obtained close to the optimal scaling behaviour of Grover's algorithm. In case of $d \leq 2$, the evolution operator arising from the massless Dirac operator is infrared divergent (as $\int d^d k / k^2$ in the continuum formulation). That slows down spatial search algorithms by logarithmic factors in $d = 2$ [2–4], compared to the optimal scaling form, and our algorithm suffers the same fate. In this article, we modify our algorithm by introducing an effective mass in the Dirac evolution operator, and demonstrate how that overcomes the infrared hurdles and improves the scaling behaviour.

We study the specific case of search for a marked vertex on a square lattice with $N = L^2$ vertices. In our algorithmic strategy [5], the free Dirac Hamiltonian,

$$H_{\text{free}} = -i\vec{\alpha} \cdot \vec{\nabla} + \beta m . \quad (1)$$

diffuses the amplitude distribution around the lattice, while the potential attracting the amplitude distribution towards the marked vertex provides the binary oracle,

$$\begin{aligned} V &= V_0 \delta_{\vec{x},0} , \quad e^{-iV_0\tau} = -1 \\ \Rightarrow R &= e^{-iV\tau} = I - 2|\vec{0}\rangle\langle\vec{0}| . \end{aligned} \quad (2)$$

Up on discretising the Hamiltonian according to the staggered lattice fermion formalism [6], the anticommuting

Dirac matrices are reduced to location dependent signs,

$$\alpha_n \longrightarrow \prod_{j=1}^{n-1} (-1)^{x_j} , \quad \beta \longrightarrow \prod_{j=1}^2 (-1)^{x_j} \beta . \quad (3)$$

To construct discrete and local time evolution, we need to exponentiate the terms in the Hamiltonian such that the resultant unitary operators are local. The mass and potential terms are single vertex local terms, and so can be exponentiated easily. To obtain local exponential of the kinetic term connecting neighbouring vertices, we separate the “odd” and “even” parts of the Hamiltonian on the bipartite square lattice, and exponentiate each block-diagonal Hermitian part separately [7]:

$$H_{\text{free}} = H_o + H_e + H_m , \quad U = \exp(-iH\tau) . \quad (4)$$

The 4×4 blocks of the Hamiltonian, corresponding to hypercubes with coordinate labels $\{0,1\}^{\otimes 2}$, are (in terms of tensor products of Pauli matrices)

$$H_o^B = -\frac{1}{2}(I \otimes \sigma_2 + \sigma_2 \otimes \sigma_3) , \quad (5)$$

and $H_e^B = -H_o^B$ when operating on a hypercube with all coordinates flipped in sign. The factors appearing in the Trotter's formula for the discrete time evolution operator then become

$$U_{o(e)} = cI - is\sqrt{2}H_{o(e)} , \quad (6)$$

with $s = \sin(\tau/\sqrt{2})$ and $|c|^2 + |s|^2 = 1$. We choose the unitary quantum walk operator to be

$$W = U_e U_o = \exp(-i(H_o + H_e)\tau) + O(\tau^2) . \quad (7)$$

Our initial state for the spatial search problem is the unbiased uniform superposition state, $|s\rangle = \sum_x |\vec{x}\rangle / \sqrt{N}$. For $m = 0$, our algorithm alternates between the oracle and the walk operators, yielding the evolution

$$\psi(\vec{x}; t_1, t_2) = [W^{t_1} R]^{t_2} \psi(\vec{x}; 0, 0) . \quad (8)$$

*Electronic address: adpatel@cts.iisc.ernet.in

†Electronic address: ksraghu@yahoo.com

‡Electronic address: aminoorrahaman@yahoo.com

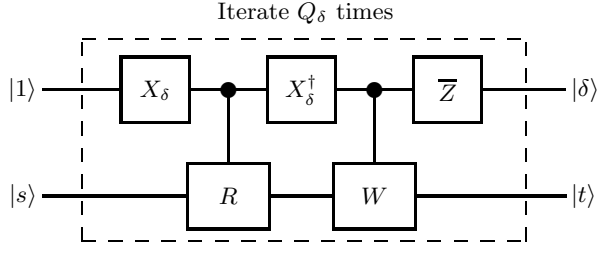


FIG. 1: Logic circuit diagram for Tulsi's controlled quantum spatial search algorithm. R and W are the binary oracle and the massless Dirac walk operator respectively. We use the generalisation with $W \rightarrow W^{t_1}$.

Here t_2 is the number of oracle calls, and t_1 is the number of walk steps between the oracle calls. Both have to be optimised, depending on the size of the lattice, to find the quickest solution to the search problem.

With iterative unitary operations, spatial search algorithms produce results periodic in time. Unlike Grover's algorithm, however, the maximum probability of being at the marked vertex, P , does not reach the value 1. Augmenting the algorithm by the amplitude amplification procedure [8], the marked vertex can be found with probability $\Theta(1)$, and the overall complexity of the algorithm is then characterised by the effective number of oracle calls t_2/\sqrt{P} .

II. IMPROVING THE ALGORITHM

We have argued [1] that spatial search in d dimensions obeys two lower bounds,

$$t_2 \geq \max\{dN^{1/d}, \pi\sqrt{N}/4\}, \quad (9)$$

following from distinct physical principles of special relativity and unitarity respectively. The bounds cross in the critical dimension $d = 2$, where logarithmic corrections to scaling behaviour are expected in analogy with critical phenomena in statistical mechanics. Such logarithmic slow down factors have been observed in earlier works [2–4], and we want to suppress them as much as possible by suitably adjusting the evolution Hamiltonian.

When $m = 0$, the quantum random walk provides the fastest diffusion, minimising t_2 . But $m = 0$ also makes the evolution operator infrared divergent in two dimensions, which spreads out the amplitude distribution in the Hilbert space too much and decreases P . Introduction of $m \neq 0$ would slow down the diffusion, but would also regulate the infrared divergence through $k^2 \rightarrow k^2 + m^2$. For small enough m , the diffusion speed (and hence t_2) may not change much, but substantial modification of the contribution of $|\vec{k}| \lesssim m$ modes can alter the behaviour of P . In such a case, an optimal value of m can be obtained by trading off the increase in t_2 against the increase in P . For a finite lattice, the lattice size acts as the infrared

cutoff, and so the optimal value of m is expected to be a function of the database size N .

Tulsi constructed an algorithm possessing the above described properties, by controlling the evolution operators using an ancilla qubit [4]. His scheme is illustrated in Fig.1, where the ancilla operators are

$$X_\delta = \begin{pmatrix} \cos \delta & \sin \delta \\ -\sin \delta & \cos \delta \end{pmatrix}, \quad \bar{Z} = \begin{pmatrix} -1 & 0 \\ 0 & 1 \end{pmatrix}, \quad (10)$$

and the algorithm evolves the initial state $|1\rangle \otimes |s\rangle$ to the target state $|\delta\rangle \otimes |t\rangle$ with $|\delta\rangle = X_\delta^\dagger |1\rangle$.

For $\delta = 0$, Tulsi's algorithm reduces to spatial search using the massless Dirac walk operator, which finds the marked vertex with probability $P_0 = \Theta(1/\log N)$ using $Q_0 = \Theta(\sqrt{N \log N})$ oracle calls [2, 3]. Tulsi showed that with $\cos \delta = \Theta(1/\sqrt{\log N})$, the algorithm increases the probability of finding the marked vertex to $P_\delta = \Theta(1)$ without changing the scaling of oracle calls $Q_\delta = \Theta(\sqrt{N \log N})$ [4]. More explicitly, the algorithm largely confines the evolution of the quantum state to a two-dimensional subspace of the N -dimensional Hilbert space, whereby

$$P_\delta = \frac{1}{2^d B_\delta^2}, \quad Q_\delta = \frac{\pi B_\delta \sqrt{N/2^d}}{4 \cos \delta}, \quad (11)$$

$$B_\delta^2 = 1 + (B^2 - 1) \cos^2 \delta. \quad (12)$$

Here $B \equiv B_0 = \Theta(\sqrt{\log N})$ is a second moment constructed from the eigenspectrum of W , and characterises the infrared divergence of the problem. We have also included explicit factors of 2^d that are appropriate for spatial search with staggered fermions, where different vertices of an elementary hypercube correspond to different degrees of freedom, and essentially only the degree of freedom corresponding to the marked vertex participates in the search process [1].

The optimal value of the ancilla control parameter is obtained by minimising the algorithmic complexity (where factors of 2^d cancel):

$$(\cos \delta)_{\text{opt}} = (B^2 - 1)^{-1/2} \approx 1/B, \quad (B_\delta^2)_{\text{opt}} = 2, \quad (13)$$

$$\left(\frac{Q_\delta}{\sqrt{P_\delta}}\right)_{\text{min}} = \frac{\pi \sqrt{N} B}{2}. \quad (14)$$

A. Rephrasing of Tulsi's Algorithm

Tulsi's algorithm is not presented in the Dirac operator language—rather the ancilla qubit is introduced in an ad hoc manner. Here we relate its ingredients to the well-known properties of the Dirac operator, in order to gain some physical insight in to its dynamical behaviour.

Consider two species of Dirac particles: one with only the mass term in the Hamiltonian (completely at rest),

and the other with only the kinetic term in the Hamiltonian (fully relativistic). Associating the species index with the ancilla value, we have

$$\begin{aligned} H_{\text{free}}^{(0)} &= |0\rangle\langle 0| \otimes H_m, \\ H_{\text{free}}^{(1)} &= |1\rangle\langle 1| \otimes (H_o + H_e). \end{aligned} \quad (15)$$

Now, pick m to give the farthest unitary evolution, i.e.

$$e^{-i\beta m\tau} = -1. \quad (16)$$

(The sign provided by β does not matter in this case.) With these choices, the two species evolve independently with maximum evolution contrast. The total Hamiltonian then yields the second half of the iteration in Tulsi's algorithm—schematically,

$$\begin{aligned} e^{-i(H_{\text{free}}^{(0)} + H_{\text{free}}^{(1)})\tau} &\longrightarrow \begin{pmatrix} -1 & 0 \\ 0 & W \end{pmatrix} \\ &= (c_1 W) \bar{Z} = \bar{Z} (c_1 W). \end{aligned} \quad (17)$$

The first half of the iteration in Tulsi's algorithm is a controlled oracle, conditioned on the state $|\delta\rangle$, i.e.

$$(c_\delta R) = X_\delta^\dagger (c_1 R) X_\delta. \quad (18)$$

For the vertices $\vec{x} \neq 0$ without the potential, it is the identity operation. That lets the “|0>” species remain at rest while the “|1>” species diffuses at full speed, and there is no mixing between the two. A consequence is that the amplitudes $|0\rangle \otimes |\vec{x} \neq 0\rangle$ do not change from their initial value zero. They neither mix with the amplitudes $|1\rangle \otimes |\vec{x} \neq 0\rangle$ nor get any contribution from the amplitude $|0\rangle \otimes |\vec{x} = 0\rangle$ by a walk step.

The potential at $\vec{x} = 0$ couples the two species, as per

$$(c_\delta R)_{\vec{x}=0} = Z X_{2\delta} = \bar{Z} X_{2\delta-\pi}. \quad (19)$$

As a result, when the diffusing “|1>” species reaches the marked vertex, part of it gets converted to the “|0>” species and stops diffusing. At the next iteration, part of the “|0>” species gets reconverted to the “|1>” species and starts diffusing again. The net effect is that the conversions reduce the number of W -operations for walks when they pass through the marked vertex. The state $|0\rangle \otimes |\vec{x} = 0\rangle$ thus acts like a trap, and the concentration of the quantum state amplitude at the marked vertex increases P_δ . Since the conversion between species pauses the walk, it can be interpreted as an effective mass, but this effective mass is unusual in the sense that it appears only at the marked vertex.

The determination of the optimal value of δ requires an analysis of the eigenspectrum of the operator W . As shown by Tulsi [4], when the evolution is largely confined to a two-dimensional subspace of the Hilbert space, $(\cos \delta)_{\text{opt}} = \Theta(1/\sqrt{\log N})$ and $\delta \approx \pi/2$. Note that for $\delta = \pi/2$, Eq.(19) implies that the two species decouple completely. So the mixing of species per iteration is tiny. Also, the target state is essentially the trap state, $|\delta\rangle \otimes |\vec{x} = 0\rangle \approx |0\rangle \otimes |\vec{x} = 0\rangle$, which is reached from the initial state $|1\rangle \otimes |s\rangle$ with $\Theta(1)$ probability by accumulating the mixing of species over many iterations.

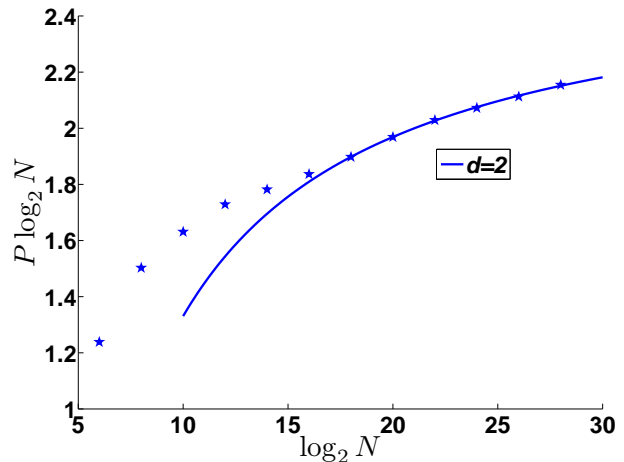


FIG. 2: Peak probability at the marked vertex as a function of database size and without ancilla control. We used $t_1 = 3$, and the curve is the fit $P \log_2 N = a_1 + (b_1 / \log_2 N)$.

TABLE I: Fit parameters for peak probability without ancilla

s	t_1	L	a_1	b_1	Error
$\frac{1}{\sqrt{2}}$	3	512—16384	2.607	-12.76	2.42×10^{-3}

III. SIMULATION RESULTS

We carried out numerical simulations of our quantum spatial search algorithm, with a single marked vertex, and both with and without ancilla control. The choice to keep the walk matrices (U_o and U_e), as well as the ancilla operators (X_δ and \bar{Z}), real was convenient for numerical simulations.

As in the case of our $d > 2$ simulations [1], we first scanned for the best values of the parameters s and t_1 to optimise the algorithm. We again found that correlated $s - t_1$ pairs simultaneously maximise P and minimise the corresponding value of t_2 . With increasing t_1 , P increases somewhat and t_2 decreases slightly, but they are minor improvements. The major difference was observed in the dependence of the optimal parameters on the lattice size. Without ancilla control and for fixed t_1 , the optimal P decreases and the optimal s increases with increasing L . The variable $\theta = \sqrt{2} t_1 \sin^{-1} s = t_1 \tau$ is somewhat larger than π (the value found in case of $d > 2$ [1]), and increases with increasing L . This dependence on the lattice size is a consequence of the infrared divergence, whereby all the spatial modes do not contribute to the search process with equal strength. On the other hand, with ancilla control and for fixed t_1 , the optimal values of P and s show little dependence on L . The variable θ is still a bit larger than π , but it is more or less a constant. These features indicate that the infrared divergence of the spatial modes is brought under control.

For concreteness in further analysis, we stuck to the parameter choice $s = 1/\sqrt{2}$ and $t_1 = 3$, which is close to

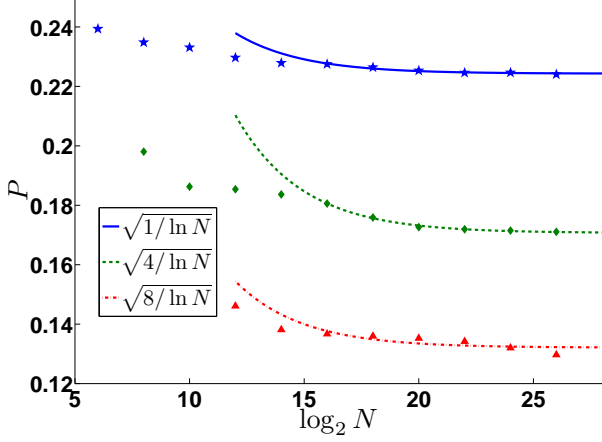


FIG. 3: Peak probability at the marked vertex as a function of database size for different values of the ancilla control parameter $\cos \delta$. We used $t_1 = 3$, and the curves are the fits $P = a_1 + (b_1/L)$.

TABLE II: Fit parameters for peak probability with ancilla

s	t_1	L	$\cos \delta$	a_1	b_1	Error	B_δ
$\frac{1}{\sqrt{2}}$	3	256—8192	$\sqrt{1/\ln N}$	0.2243	0.873	2.50×10^{-4}	1.056
			$\sqrt{4/\ln N}$	0.1717	2.536	2.47×10^{-4}	1.207
			$\sqrt{8/\ln N}$	0.1321	1.429	1.53×10^{-3}	1.376

the optimal choice, both with and without ancilla control. It is not easy to theoretically estimate B , and hence determine the ideal proportionality constant between the control parameter $\cos \delta$ and $1/\sqrt{\log N}$. To figure that out numerically, we performed simulations with three different choices: $\cos \delta = \sqrt{1/\ln N}$, $\sqrt{4/\ln N}$, $\sqrt{8/\ln N}$.

Our results for the dependence of the peak probability on the lattice size are displayed in Figs.2 and 3. As anticipated, P decreases logarithmically as $1/\log N$ without ancilla control, and asymptotically approaches a constant with ancilla control. Even the behaviour of the subleading correction changes from $1/\log L$ without ancilla control to $1/L$ with ancilla control, reconfirming that ancilla control indeed eliminates infrared divergence of P . The values of our fit parameters are presented in Tables I and II, where error refers to the r.m.s. deviation of the data from the fit. In Table II, we have also included the related values of B_δ following from Eq.(11).

Next we display our results for the dependence of the number of oracle calls on the lattice size in Fig.4. As expected, t_2 increases with decreasing $\cos \delta$, as species conversions slow down the walk. But this slow down is only by a multiplicative factor, and $t_2/\sqrt{N \log N}$ asymptotically approaches a constant in all cases. Furthermore, the subleading correction is well parametrised as $1/L$, suggesting that t_2 is less affected by infrared divergence of the problem than P is. There is some oscillatory pattern in the data [11], while the approach to the asymp-

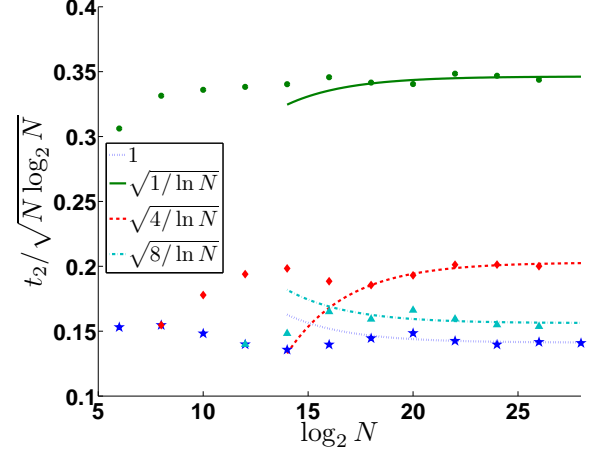


FIG. 4: Number of oracle calls as a function of database size for different values of $\cos \delta$. We used $t_1 = 3$ and the curves are the fits $t_2/\sqrt{N \log_2 N} = a_2 + (b_2/L)$.

TABLE III: Fit parameters for search oracle calls for various values of the ancilla control parameter $\cos \delta$

s	t_1	L	$\cos \delta$	a_2	b_2	Error	B_δ
$\frac{1}{\sqrt{2}}$	3	512—16384	1	0.1412	2.755	2.25×10^{-3}	—
		512—8192	$\sqrt{1/\ln N}$	0.3463	-2.782	2.41×10^{-3}	1.059
		512—8192	$\sqrt{4/\ln N}$	0.2030	-8.977	1.54×10^{-3}	1.242
		512—8192	$\sqrt{8/\ln N}$	0.1562	3.290	3.81×10^{-3}	1.351

totic behaviour becomes smoother with decreasing $\cos \delta$. The values of our fit parameters are presented in Table III. Again error refers to the r.m.s. deviation of the data from the fit, and the related values of $B_{\delta \neq 0}$ following from Eq.(11) are included.

For a more elaborate comparison with Tulsi's analysis, we check whether our fit parameters obey Eq.(11) parametrised in terms of the second moment B . Without ancilla control, values of P and t_2 should be related by $(4a_1)^{-1/2} = 8a_2/\pi$. That leads to the comparison $0.31 \leftrightarrow 0.36$, which is quite reasonable. Stating it another way, our estimates of B vary from $0.31\sqrt{\log_2 N}$ to $0.36\sqrt{\log_2 N}$. Possible reasons for the discrepancy are: (a) contribution of subleading terms neglected in Tulsi's analysis (e.g. from the states outside the two-dimensional subspace used in the evolution), (b) the notorious difficulty in accurately extracting parameters from asymptotically logarithmic fits.

With ancilla control, the values of B_δ in Tables II and III match well; control over infrared divergence definitely helps in extraction of the scaling behaviour. They give estimates of B varying from $0.27\sqrt{\log_2 N}$ to $0.31\sqrt{\log_2 N}$. As per Eq.(13), therefore, the optimal choice for the ancilla control parameter would be

$$(\cos \delta)_{\text{opt}} \approx 3.5\sqrt{1/\log_2 N} \approx \sqrt{8.5/\ln N}. \quad (20)$$

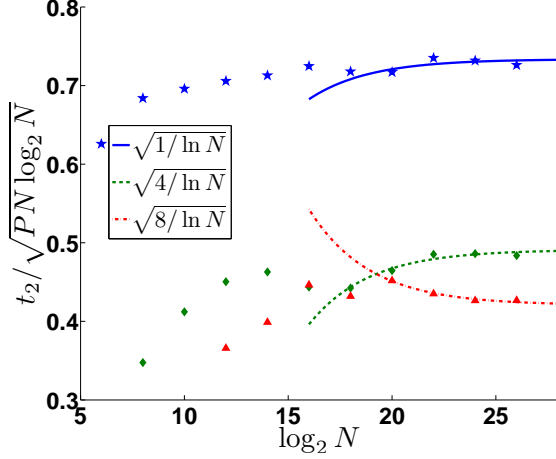


FIG. 5: Effective number of oracle calls as a function of database size for different values of the ancilla control parameter $\cos \delta$. We used $t_1 = 3$ and the curves are the fits $t_2/\sqrt{PN \log_2 N} = a_3 + (b_3/L)$.

TABLE IV: Fit parameters for the algorithmic complexity for various values of the ancilla control parameter $\cos \delta$

s	t_1	L	$\cos \delta$	a_3	b_3	Error
$\frac{1}{\sqrt{2}}$	3	1024—8192	$\sqrt{1/\ln N}$	0.7336	-13.06	5.31×10^{-3}
			$\sqrt{4/\ln N}$	0.4911	-24.30	4.03×10^{-3}
			$\sqrt{8/\ln N}$	0.4207	31.24	1.53×10^{-3}

Our numerical simulations had database sizes varying from $N = 2^{12}$ to 2^{26} . So in order to maintain $\cos \delta \leq 1$, we had to restrict the proportionality constant between $\cos \delta$ and $\sqrt{1/\ln N}$. Nevertheless, our largest parameter choice, $\cos \delta = \sqrt{8/\ln N}$, is close to optimal.

Finally, we combine the results for P and t_2 , to look at the scaling behaviour of the algorithmic complexity t_2/\sqrt{P} . Without ancilla control, the effective number of

oracle calls scales as $\sqrt{N} \log N$, with $a_2/\sqrt{a_1}$ being the proportionality constant. Our results with ancilla control are displayed in Fig. 5, together with the fit parameters in Table IV. The scaling of the effective number of oracle calls is improved to $\sqrt{N \log N}$, with the proportionality constant a_3 essentially the same as $a_2/\sqrt{a_1}$. Due to the oscillatory pattern in the data and non-negligible subleading corrections, our results are inadequate to numerically optimise a_3 . On the other hand, our estimates of B and Eq. (14) give $(a_3)_{\text{opt}} \approx 0.45$. That is consistent with the value for our close to optimal parameter choice $\cos \delta = \sqrt{8/\ln N}$, and hence we infer our best algorithmic complexity to be $t_2/\sqrt{P} \approx 0.45 \sqrt{N \log_2 N}$.

IV. SUMMARY

For the spatial search problem, $d = 2$ is the critical dimension where infrared divergences appear. Introduction of a mass term in the evolution operator can suppress infrared divergences, and we have reinterpreted Tulsi's ancilla control of the spatial search algorithm as introduction of an effective mass at the marked vertex.

Our numerical results demonstrate how ancilla control improves the scaling behaviour of the spatial search algorithm in $d = 2$. In particular, they agree with Tulsi's predictions [4], and validate his analysis criterion that the evolution of the quantum state is largely confined to a two-dimensional subspace of the N -dimensional Hilbert space. The change in scaling of P with ancilla control is a clear signal for suppression of the infrared divergence. Asymptotic behaviour of t_2 does not change, however. It retains the $\sqrt{\log N}$ factor beyond the lower bounds in Eq. (9), indicating that some effect of the critical behaviour survives. It is an open question whether this is the minimal extra cost to be paid in the critical dimension for the spatial search problem, or whether it can be reduced further.

[1] A. Patel and M.A. Rahaman, arXiv:1003.0065.
[2] A. Ambainis, J. Kempe and A. Rivosh, Proceedings of ACM-SIAM SODA'05 (ACM Press, New York, 2005), p. 1099, arXiv:quant-ph/0402107.
[3] A.M. Childs and J. Goldstone, Phys. Rev. A 70 (2004) 042312, arXiv:quant-ph/0405120.
[4] A. Tulsi, Phys. Rev. A 78 (2008) 012310, arXiv:0801.0497; See also his Ph.D. Thesis, Indian Institute of Science, Bangalore (2009).
[5] L.K. Grover, Pramana 56 (2001) 333, arXiv:quant-ph/0109116.
[6] L. Susskind, Phys. Rev. D 16 (1977) 3031.
[7] A. Patel, K.S. Raghunathan and P. Rungta, Proceedings of the Workshop on Quantum Information, Computation and Communication (QICC-2005), IIT Kharagpur, (Al-

lied Publishers, 2006), p. 41, arXiv:quant-ph/0506221.
[8] G. Brassard, P. Hoyer, M. Mosca and A. Tapp, in *Quantum Computation and Information*, AMS Contemporary Mathematics Series Vol. 305, eds. S.J. Lomonaco and H.E. Brandt (AMS, Providence, 2002), p. 53, arXiv:quant-ph/0005055.
[9] C. Zalka, Phys. Rev. A 60 (1999) 2746, arXiv:quant-ph/9711070.
[10] C. Bennett, E. Bernstein, G. Brassard and U. Vazirani, SIAM J. Comput. 26 (1997) 1510, arXiv:quant-ph/9701001.
[11] We do not properly understand this, but it perhaps indicates a second relevant length scale in the problem.